Proceedings of the 2009 IEEE International Conference on Systems, Man, and Cybernetics
San Antonio, TX, USA - October 2009

Haptic Interface in UAV Tele-operation using Force-stiffness Feedback

T. Mung Lam, Max Mulder and M. M. (René) van Paassen

***Abstract*—This study investigates the use of force-stiffness feedback, i.e., a combination of force offset and extra spring load, in UAV tele-operation with transmission time delay. The goal was to further increase the level of safety of tele-operation with a reduction in operator workload with respect to force feedback, i.e., using force offset alone. A theoretical analysis is given of using force-stiffness feedback to improve collision avoidance. Wave variables are included to reduce time delay effects. An experiment was conducted to investigate the effects of force-stiffness feedback on safety of operation, operator performance, control activity, and workload. Results indicate that force-stiffness feedback improves the haptic interface with respect to force feedback alone. Safety of tele-operation increases without increasing operator workload with respect to force feedback.**

***Index Terms*—Tele-operation, haptics, unmanned aerial vehicles.**

I. Introduction

In the tele–operation of an uninhabited aerial vehicle (UAV), operators are physically separated from the vehicle. The information provided at the ground station is usually visual with limited field of view. Additionally, in case of using satellite communication between a UAV and a ground station, considerable signal transmission time delays are involved. All these will result in poor situation awareness, poor efficiency, and unsafe tele-operation[1], [2].

Previous studies have shown that haptic feedback on a control device, i.e., information through the sense of touch, can complement the visual information to increase the efficiency and safety of tele-operation [3], [4]. For collision avoidance in UAV tele-operation, the focus of our study, Lam, Mulder, and Van Paassen investigated the effectiveness of force feedback, i.e., force offsets on the control device, in helping operators to control the UAV through an obstacle-laden environment [5]. Virtual repulsive forces generated by an artificial force field (AFF) [6] were used by the haptic control device to provide operators with information about the environment. Results showed that the number of collisions decreased significantly, but workload increased with respect to the case of no haptic feedback. High workload corresponded to large variations in the force feedback.

When signal transmission time delays exist in a bilateral system such as haptic feedback on the control device, delayed repulsive forces cannot be ignored by the operator and will be considered as external disturbances. Research has reported that even small time delays can already cause control difficulties and instabilities in tele-operation [1], [3]. In another study by Lam et al. the effects of force feedback in UAV tele-operation with a transmission time delay was investigated to see if it would indeed lead to a decrease in safety and increase in workload [7]. Results showed that with a combination of force feedback with the wave variables transformation introduced by Niemeyer [8], the level of safety increased significantly with respect to a situation without haptic feedback. Workload was still higher than in the case of no haptic feedback, however [7]. Additionally, large variations in force feedback and stick deflection rates corresponded to high workload.

In a third study by Lam et al. the use of stiffness feedback, i.e., spring load modification, was investigated without considering time delay. Here it was found that with stiffness feedback operator workload decreased with respect to the no haptic feedback case, while an equivalent level of safety was achieved with respect to the force feedback case [9]. Again, in this study it was found that large variations in force feedback corresponded to high workload.

The goal of this study was to improve haptic feedback for UAV tele-operation with time delay in the communication link using a combination of force feedback and stiffness feedback, which is referred to as force-stiffness feedback. Our main hypothesis was that with force-stiffness feedback the level of safety can be improved while reducing operator workload at the same time. Based on the findings in previous research [5], [7], [9], it was assumed that workload can be caused by large variations in the force feedback, which can in turn be caused by large intensities of the repulsive forces. The approach was to reduce the force offsets while providing sufficient repulsive forces for effective collision avoidance.

This paper describes a theoretical and experimental investigation of the use of force-stiffness feedback in the UAV tele-operation in the horizontal plane with a time delay. Section II describes some possible representations of haptic feedback that provide repulsive forces: force feedback, stiffness feedback, stiffness-force feedback, and force-stiffness feedback. Section III describes an analysis of the force-stiffness feedback using offline simulations to show collision avoidance effectiveness. Section IV discusses a human-in-the-loop experiment to investigate the effects of force-stiffness feedback in UAV tele-operation with time delay, regarding safety, operator performance, control activity, and workload. The paper ends with a discussion on the results and conclusions in Sections V and VI, respectively.

II. Haptic feedback

This section describes possible representations of haptic feedback that provide repulsive forces on a control device. Our study uses a side stick as the haptic control device.

978-1-4244-2794-9/09/$25.00 ©2009 IEEE

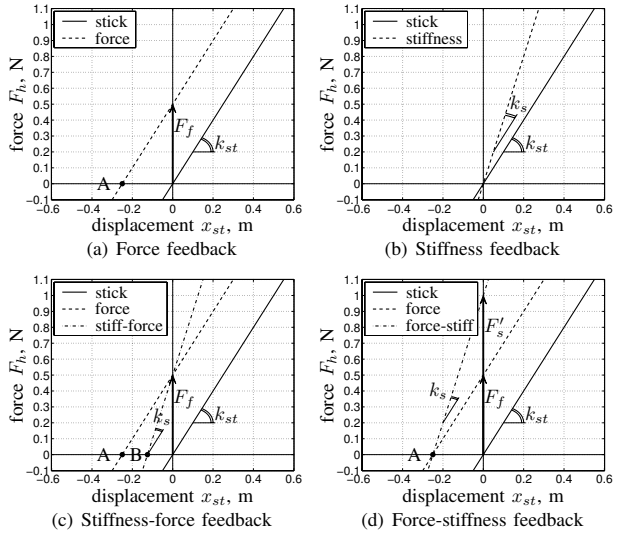

(a) Force feedback (b) Stiffness feedback (c) Stiffness-force feedback (d) Force-stiffness feedback

Fig. 1. Force-displacement relations of various haptic feedback methods.

A. Force feedback

Force feedback applies a force offset on the stick. The human operator perceives the reaction force from the stick dynamics and the external force offset. Assuming the stick is displaced to a certain position, x_{st}, then the total exerted force by the operator, i.e., the force on the hand, F_h, is written as:

$$\begin{aligned} F_h &= F_{st} + F_f, \\ F_h &= k_{st}x_{st} + F_f, \end{aligned} \tag{1}$$

with F_{st}, k_{st}, and F_f representing the reaction force from the stick, the stick spring constant, and the external force offset, respectively.

Fig. 1(a) shows that due to the force offset, the stick will have a non-zero neutral position (A), i.e., position where the stick is in equilibrium in the absence of external forces. When the stick is released, $F_h = 0$, repulsive forces can still exist and the stick actively deflects away from the direction with a possible collision: $x_{st} = -F_f/k_{st}$. Based on the findings by Lam et al. [7], it is hypothesized that the amplitude of variations in stick motions due to neutral position changes can contribute to workload. Decreasing the force offset would be a solution, but the repulsive forces may then be considered as too low by operators.

B. Stiffness feedback

Stiffness feedback involves addition of an extra spring load, k_s, to the fixed stick dynamics' spring constant k_{st}. The repulsive force only provides an impedance to the operator exerted deflection. It does not actively deflect the stick away from a possible collision. The total force on the hand in this situation can be written as:

$$\begin{aligned} F_h &= F_{st} + F_s, \\ F_h &= k_{st}x_{st} + k_s x_{st}, \end{aligned} \tag{2}$$

with F_s representing the force due to an extra spring load k_s. Fig. 1(b) shows that the slope of the force-excursion relation increases due to the extra spring load. A zero displacement leads to zero repulsive force. For small displacements the repulsive forces would be small and human operators may not perceive sufficient haptic information.

Hence, on the one hand it is required that the haptic device is capable of actively deflecting away from a possible collision, with only small overshoot from the zero displacement to prevent control problems. On the other hand, the haptic feedback should be able to provide large resistance when the stick is deflected in the direction with high risk of collision. These desired properties can be obtained with a combination of force feedback with stiffness feedback. Two possible combinations will be discussed below.

C. Stiffness-force feedback

Based on stiffness feedback alone, the lack of active stick repulsive motions or the insufficient force intensity with small stick displacements can be resolved by adding a small force offset, which will be referred to as stiffness-force feedback. The total exerted force by the human operator is then written as:

$$\begin{aligned} F_h &= F_{st} + F_s + F_f, \\ F_h &= k_{st}x_{st} + k_s x_{st} + F_f, \end{aligned} \tag{3}$$

This system was used by Lam et al. [9], and resulted in lower workload and equivalent level of safety with respect to force feedback alone. The drawback of this system, however, is that when the stiffness increases, the desired small offset of the neutral position, (A), by the force feedback will decrease, which results in (B), see Fig. 1(c). This would reduce operator workload but when (A) already corresponds to a small repulsive force, a further reduction of the neutral position will lead to a force that can be experienced as too low by operators.

D. Force-stiffness feedback

Based on force feedback alone, reducing the force offset to get the desired small neutral position offset may lead to repulsive forces that are considered as too low or insufficient for effective collision avoidance. This can be compensated for by adding extra spring load. The desired property of force feedback, i.e., a non-zero neutral position to actively move the stick away from the direction with a possible collision, must be maintained. Therefore, the addition of the extra spring load here requires a compensation for its decreasing effect on the neutral position offset [10]. The total exerted force can then be written as:

$$F_h = F_{st} + (F_s + F'_s) + F_f, \tag{4}$$

with F'_s representing the force offset to account for the effect of stiffness feedback in order to maintain the same neutral position offset (A). From Fig. 1(d) it can be derived that this extra force offset can be calculated using the force feedback

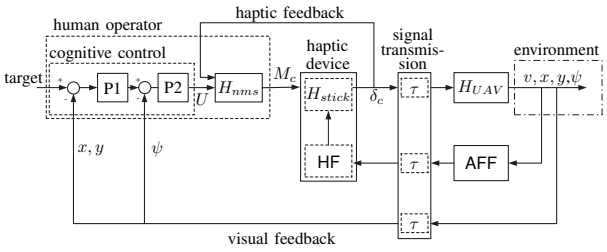

Fig. 2. Schematic representation of a closed-loop autonomous system.

TABLE I
OPERATOR MODEL PROPORTIONAL GAINS AND FORCE-STIFFNESS FEEDBACK FORCE GAINS (NM) AND STIFFNESS GAINS (NM/RAD). THE SUBSCRIPTS p AND r REPRESENT THE ROLL (LATERAL) AND PITCH (LONGITUDINAL) DIRECTIONS, RESPECTIVELY.

Trajectory	human		haptic feedback			
			lateral		longitudinal	
	P1	P2	G_{f_r}	G_{s_r}	G_{f_p}	G_{s_p}
A	0.09	2.3	0.45	6.38	0.45	7.29
B	0.05	1.7	0.45	15.00	0.45	17.14
C	0.02	9.0	0.45	0.00	0.45	4.71
D	0.02	0.9	0.45	3.38	0.45	4.29

F_f, the extra spring load k_s, and the control device spring constant k_{st}: $F'_s = (k_s/k_{st})F_f$.

Although the resulting force-stiffness feedback results in the same neutral position as with force feedback alone, it offers better haptic feedback design. Force-stiffness feedback enables the presentation of large repulsive forces to represent risk of potential collision, but does not result in excessive position offsets. Additionally, the small force offset will not further decrease with increasing stiffness due to F'_s. Hence, this system is hypothesized to be a potential candidate to improve haptic feedback for collision avoidance in UAV tele-operation.

III. SIMULATION

A UAV tele-operation simulation will be described, using an artificial force field (AFF) for generating haptic feedback to improve collision avoidance [6]. Our goal was to investigate whether force-stiffness feedback can be used for tele-operation of a UAV through an obstacle-laden environment. Important aspects are the UAV motion and collision avoidance effectiveness.

A. Setup

Fig. 2 shows a schematic representation of the closed-loop model. It contains an operator model including a neuromuscular system, a stick control device, a UAV, and an artificial force field. Below, the components of the model will be described in more detail.

The human operator is a proportional controller on the position error (P1) and heading error (P2) with respect to a fixed two-dimensional target position. The output of the operator cognitive control, U, will cause the neuromuscular system, H_{nms}, to exert a moment input, M_c, on the control device. The H_{nms} is a two-dimensional mass-spring-damper system modeled for our control device, a side stick [11].

The stick, H_{stick}, is modeled as a mass-spring-damper system that is identical in the lateral and longitudinal direction with a moment of inertia $I_{st} = 0.01$ kgm^2, a damping coefficient $B_{st} = 0.2$ Nms/rad, and a spring constant $K_{st} = 2$ Nm/rad. The stick deflection, δ_c, serves as a rate command for the UAV model. Note that here the human-stick interaction is defined using moments and deflections, rather than forces and displacements.

The UAV, H_{UAV}, is assumed to be a control-augmented helicopter. A longitudinal stick deflection represents a velocity command in the longitudinal direction, with second order dynamics, 1/((0.3s+1)(0.18s+1)). A lateral stick deflection represents a yaw-rate command with first order dynamics, 1/(0.2s+1). The UAV has a maximum velocity of 5 m/s and a maximum acceleration of 1 m/s^2. The UAV has a circular protection zone with a radius of 1.6 m.

An AFF from [6], the Parametric Risk Field, is used to map obstacles to repulsive forces. The output of the AFF in the longitudinal and lateral direction is a dimensionless risk value, limited to 1, which is converted to a force offset and extra spring load using gains G_f and G_s, respectively.

The control input and haptic feedback are subjected to a fixed transmission time delay $\tau = 0.2$ s. For haptic feedback, wave variables are used with wave impedance $b = 0.3$ Ns/m to reduce time delay effects [7]. The visual feedback is also subjected to the same time delay; no wave variables are applied to this feedback channel, however, which is a common practice.

Three haptic feedback conditions (HF) are evaluated. First, force feedback with $G_f = 1.5$ Nm is used, a representative case when considering an operator's exerted moment pushing the stick to the limited deflection. Second, a reduced force feedback with $G_f = 0.45$ Nm (30%) is used to reduce force offsets. Third, force-stiffness feedback is used, i.e., a combination of the reduced force feedback with stiffness feedback. The operator gains and the force-stiffness feedback gains for the lateral (G_{f_r}, G_{s_r}) and longitudinal (G_{f_p}, G_{s_p}) directions are summarized in Table I.

The same trajectories were used as in Lam et al. [6]. Representative maneuvers, such as making a sharp turn, a passage through narrow corridors, stopping before a dead-end, and moving through a passage with irregularities in the wall, were used to test the collision avoidance effectiveness of reduced force feedback and force-stiffness feedback with time delay.

B. Results

The simulation results are shown in Fig. 3. Force feedback enables the UAV to reach the targets without collisions. Reduced force feedback leads to collisions in trajectories B, C, and D, see Fig. 3(b), indicating that the feedback provided is insufficient to safely guide the UAV through these scenarios. Combining stiffness feedback with the reduced force feedback enables the UAV to move through the environment without collisions again, see Fig. 3(c).

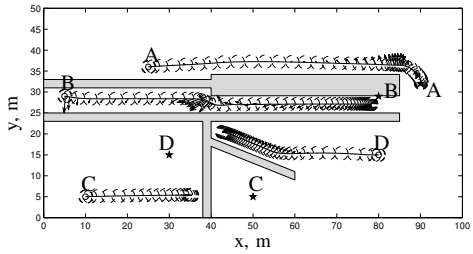

(a) force feedback

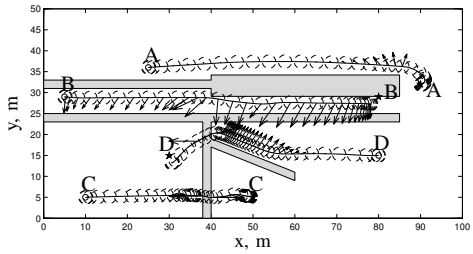

(b) reduced force feedback

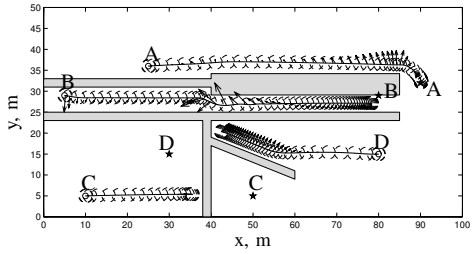

(c) force-stiffness feedback

Fig. 3. Simulation results of the closed-loop system. The '$\circ$' and '$\star$' indicate the start and target positions, respectively. The dashed circles and arrows represent the UAV positions and the repulsive forces with a 1 second interval, respectively. The trajectories are indicated by a letter.

Force-stiffness feedback enables small force offsets, while providing sufficient repulsive force intensity due to the addition of extra spring load. The small force offsets are desired in a flight through a narrow corridor or between closely-spaced obstacles (trajectory B). The resulting small repulsive stick motions should be enough to avoid a collision without leading to a possible collision with other obstacles in the vicinity during the avoidance maneuver. The variations in stick motions would then be small and therefore, workload is predicted to be lower with force-stiffness feedback. To investigate whether operator workload indeed reduces with force-stiffness feedback, a human-in-the-loop experiment is required.

IV. Experiment

An experiment was conducted to investigate the effects of force-stiffness feedback in UAV tele-operation. The investigation focused on collision avoidance effectiveness, operator performance, control activity, and workload.

A. Method

1) Subjects and instructions: Eleven subjects between the age of 23 and 27 years with no previous flight experience

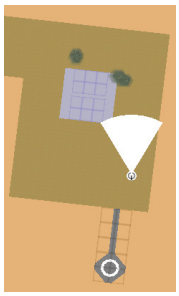

(a) 2-dimensional navigation display

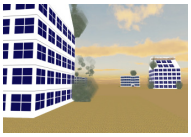

(b) 3-dimensional camera display

Fig. 4. Navigation and camera display.

participated in the experiment. A reconnaissance task in a hazardous environment was simulated. The subjects' main task was to fly a UAV in an environment with various buildings, from waypoint to waypoint. They were instructed to fly as fast as possible, and aim to fly through the center of each waypoint as accurately as possible without collisions. The waypoints were represented by smoke plumes, located in the vicinity of the buildings. When a collision occurred, subjects were notified by a loud beep and were given a penalty of 60 s during which they could not fly. After the 60 s the UAV was reset to the 'reset' initial position that will be introduced in Section IV-A4. After each run subjects were asked to rate their workload using the NASA TLX rating scale [12].

2) Apparatus: The experiment was conducted in a fixed-base flight simulator. Subjects were seated on an aircraft chair in front of an 18 inch screen, projecting a navigation display, as shown in Fig. 4(a). The image from a simulated onboard camera was projected on a wall at a distance of 2.9 m in front of the operator, as shown in Fig. 4(b). The width and height of the projected image was 1.05 m and 0.75 m, respectively, resulting in a field of view of, respectively, 20° and 15°. The display presented a camera view of 60° and 45° in the horizontal and lateral direction, respectively.

On the right-hand side of the aircraft chair an electro-hydraulic side stick was located, which was used as the haptic control device. Mass, spring, and damper stick dynamics were simulated with inertia $I_{st} = 0.01$ kgm^2, damping coefficient $B_{st} = 0.2$ Nms/rad, and spring constant $K_{st} = 2$ Nm/rad. The position of the hand contact point was located at approximately 0.09 m above the rotation axis. Both the visual and haptic channels had a fixed time delay $\tau = 0.2$ s, simulating the delayed communication link between the UAV and the ground control station.

3) UAV model: A control-augmented UAV helicopter model was used with the same dynamics and limitations as described in section III-A. The altitude was kept constant by the control augmentation at 3.5 m.

4) Independent variables: There were three levels of control configurations (CF):

NF: our baseline, no haptic feedback;
FF: force feedback with $G_{f_r} = G_{f_p} = 1.5$ Nm and wave

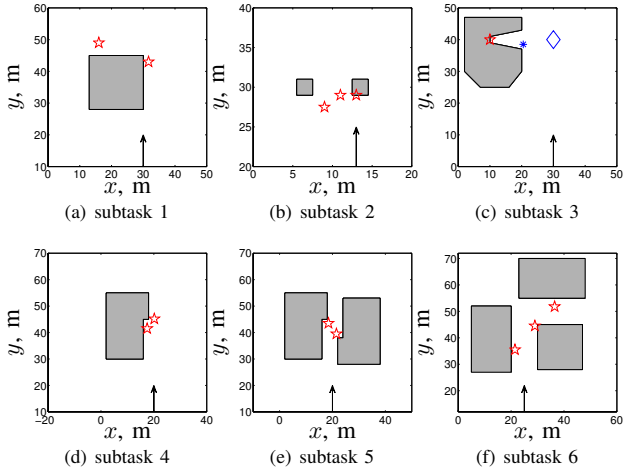

(a) subtask 1 (b) subtask 2 (c) subtask 3

(d) subtask 4 (e) subtask 5 (f) subtask 6

Fig. 5. Six subtasks used in the experiment. The arrows show the flight direction starting from the reset initial position after a collision. The stars indicate the locations of the waypoint, shown by smoke plumes.

variables ($b = 0.3$ Ns/m);

FSF: force-stiffness feedback with $G_{f_r} = G_{f_p} = 0.45$ Nm, $G_{s_r} = 3.75$ Nm/rad, $G_{s_p} = 4.29$ Nm/rad, and wave variables ($b = 0.3$ Ns/m);

Six subtasks (ST) were defined that involved different scenarios, each requiring a specific maneuver that may lead to control difficulties. The subtasks can be found in Fig. 5. The reader is referred to [9] for a detailed description of the six subtasks.

5) Trajectory: Six different trajectories were designed, each containing three different sectors [5]. Each sector contained the six subtasks in a different order. Each subject flew 3×6 = 18 runs. A typical run, but without collisions, lasted approximately six minutes.

6) Procedure: After training runs, each subject flew the 18 experiment runs in one of three randomized orders. Subjects were not informed beforehand about what haptic feedback condition they flew during the measurement runs.

7) Dependent measures: Control activity was represented by the standard deviation of the total exerted moment by the hand (σ_{M_h}) and the standard deviation of the total stick deflection rate ($\sigma_{\dot{\delta}_{tot}}$). Haptic activity was represented by the standard deviation of the total external moment by the haptic feedback ($\sigma_{M_{ext}}$). Operation efficiency was represented by the standard deviation of the UAV velocity ($\sigma_{v_{tot}}$). Operator performance was expressed by the minimum distance between the waypoint location and the center of the UAV protection zone (D_{wp}). Level of safety was expressed by the number of collisions (D_{min}). Workload was measured after each run using the NASA TLX rating scale.

B. Hypotheses

First, it was hypothesized that, in general, haptic feedback would not only result in a higher level of safety, but also in lower workload with respect to the baseline condition. The number of collisions was expected to decrease with haptic feedback. Second, it was hypothesized that force-stiffness feedback would yield a lower workload with respect to the force feedback case.

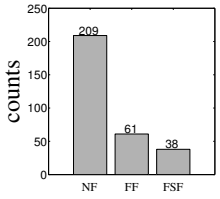

Fig. 6. Total number of collisions.

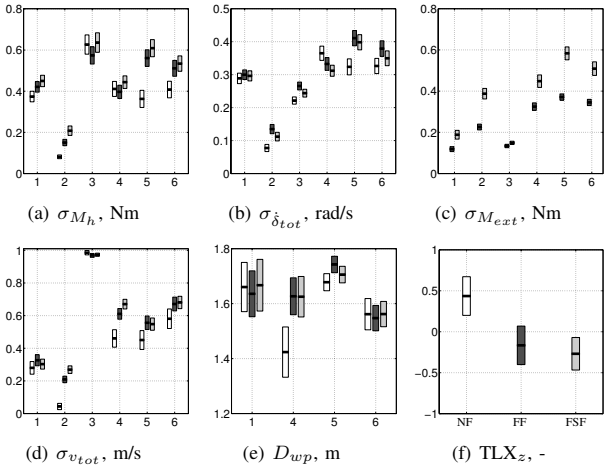

(a) σ_{M_h}, Nm (b) $\sigma_{\dot{\delta}_{tot}}$, rad/s (c) $\sigma_{M_{ext}}$, Nm

(d) $\sigma_{v_{tot}}$, m/s (e) D_{wp}, m (f) TLX_z, -

Fig. 7. Means and 95 % confidence intervals of the main dependent measures. The white, dark gray, and light gray bars represent NF, FF, and FSF, respectively. The numbers 1 to 6 on the horizontal axis correspond to the subtask numbers.

C. Results

Except for the number of collisions, only the runs without collisions were used in the analysis. A full-factorial within-subjects ANOVA was applied with post-hoc analysis using Student-Newman-Keuls (SNK, α = 0.05).

1) Number of collisions: Fig. 6 shows that the number of collisions was largest without haptic feedback. A Kruskal-Wallis test revealed a highly-significant effect of control configuration ($\chi^2 = 96.103$, $p \leq 0.01$). Force-stiffness feedback resulted in a significantly smaller number of collisions than with the force feedback condition (Mann-Whitney, $Z = -2.058$, $p = 0.040$).

2) Control activity: Control activity in terms of σ_{M_h} shown in Fig. 7(a) was largest with force-stiffness feedback and smallest without haptic feedback, a highly-significant effect (CF: $F_{2,20} = 24.454$, $p \leq 0.01$). Regarding the dependency on ST, subtask 2 resulted in the smallest σ_{M_h} and subtask 3 resulted in the largest σ_{M_h}, a highly-significant effect (ST: $F_{5,50} = 19.619$, $p \leq 0.01$). The $\sigma_{\dot{\delta}_{tot}}$ in Fig. 7(b) was lowest with the baseline condition and highest with the force

feedback, a highly-significant effect (CF: $F_{2,20} = 8.558$, $p \leq 0.01$).

3) Haptic activity: Here, the 'no haptic feedback' condition was not considered. Fig. 7(c) shows that generally $\sigma_{M_{ext}}$ was largest with force-stiffness feedback, a highly-significant effect (CF: $F_{1,10} = 53.909$, $p \leq 0.01$). In subtasks 1 and 3 $\sigma_{M_{ext}}$ was smallest, whereas it was largest in subtask 5, a highly-significant effect (ST: $F_{5,50} = 36.421$, $p \leq 0.01$).

4) UAV velocity: The $\sigma_{v_{tot}}$ shown in Fig. 7(d) was smallest without haptic feedback, a highly-significant effect (CF: $F_{2,20} = 14.287$, $p \leq 0.01$). Subtask 2 resulted in the smallest $\sigma_{v_{tot}}$, whereas subtask 3 resulted in the largest $\sigma_{v_{tot}}$, a highly-significant effect (ST: $F_{5,50} = 48.567$, $p \leq 0.01$).

5) Approach performance: The D_{wp} shown in Fig. 7(e) was best without haptic feedback, a significant effect (CF: $F_{2,20} = 3.765$, $p = 0.041$). Note that, on the other hand, many more collisions occurred than with haptic feedback as discussed in Section IV-C1. Subtasks 2 and 3 were not considered, since the smoke only served as "noise" in the visual information of the obstacle boundaries.

6) Workload: Workload was measured after a whole run and could therefore not be measured for each individual subtask. Fig. 7(f) shows the TLX z-score of the workload, where high numbers indicate high workload and vice versa. Operator workload was lowest with haptic feedback, (CF: $F_{2,20} = 5.407$, $p = 0.013$). No significant difference was found between force feedback and force-stiffness feedback.

V. Discussion

In previous research it was found that haptic feedback using force offset resulted in higher level of safety, but workload was higher than in case of no haptic feedback [5], [7], [9]. The theoretical analysis in this study showed that reducing force feedback to reduce workload would lead to more collisions. Combining stiffness feedback with the reduced force offset resulted in a much better collision avoidance.

Experimental results revealed that with haptic feedback the number of collisions and operator workload decreased significantly with respect to the baseline condition, confirming our first hypothesis. Approach performance and efficiency measured by the variations in velocity decreased with haptic feedback, but it was very small compared to the increase in safety and decrease in workload gained with haptic feedback. Second, force-stiffness feedback did not significantly reduce operator workload with respect to the force feedback condition, which contradicts our second hypothesis.

The lower workload with haptic feedback compared to the baseline condition is in contrast to the findings in previous research, where workload was highest with haptic feedback [5], [7], [9]. But in those studies no penalties or indications were given to subjects when a collision occurred. In the current experiment, each collision caused a penalty freeze of 60 s, which gave subjects more awareness of their bad performance, also without haptic feedback. Subjects became more appreciative of the haptic feedback as it helped them to increase their collision avoidance performance, even at the cost of more physical activity.

A reduction in workload with respect to force feedback was not achieved with the force-stiffness feedback in this study. It is recommended to further tune the force-stiffness feedback to find optimum settings for a further decrease in workload, while maintaining a high level of safety.

Note that force-stiffness feedback did not increase workload compared to force feedback. The variations in stick deflection rate were lower with respect to force feedback. Apparently, workload is more contributed by the variations in stick motions than by the repulsive force intensity. This indeed indicates the further potential of force-stiffness feedback, which enables smaller neutral position offsets, leading to smaller variations in stick motions.

VI. Conclusions

Haptic feedback increases the level of safety of tele-operation with a reduction in workload with respect to the no haptic feedback case. Force-stiffness feedback was found to enhance the level of safety, without increasing workload with respect to force feedback alone. It is recommended to fine-tune the feedback gains to further reduce workload, while maintaining a high level of safety.

References

[1] T. B. Sheridan, "Space teleoperation through time delay: Review and prognosis," *IEEE Transactions on Robotics and Automation*, Vol. 9, October 1993, pp. 592–606.

[2] J. S. McCarley and C. D. Wickens, "Human factors implications of UAVs in the national airspace," Aviation Human Factors Division, Savoy, Illinois, Technical report AHFD-05-05/FAA-05-01, 2005.

[3] R. J. Anderson and M. W. Spong, "Bilateral control of teleoperators with time delay," *IEEE Transactions on Automatic Control*, Vol. 34, No. 5, May 1989, pp. 494–501.

[4] B. Hannaford, L. P. Wood, D. A. McAffee, and H. Zak, "Performance evaluated of a six-axis generalized force-reflecting teleoperator," *IEEE Transactions on Systems, Man, and Cybernetics*, Vol. 21, No. 3, May/June 1991, pp. 620–633.

[5] T. M. Lam, M. Mulder, and M. M. Van Paassen, "Haptic Interface for UAV Collision Avoidance," *The International Journal of Aviation Psychology*, Vol. 17, No. 2, 2007, pp. 167–195.

[6] T. M. Lam, H. W. Boschloo, M. Mulder, and M. M. Van Paassen, "Artificial force field for collision avoidance in the UAV tele-operation," *IEEE Transactions on Systems, Man and Cybernetics, Part A*, 2009, in press.

[7] T. M. Lam, M. Mulder, and M. M. Van Paassen, "Haptic Feedback in UAV Tele-operation with Time Delay," *Journal of Guidance, Control & Dynamics*, Vol. 31, No. 6, 2008, pp. 1728–1739.

[8] G. Niemeyer and J. J. E. Slotine, "Stable adaptive teleoperation," *IEEE Journal of Oceanic Engineering*, Vol. 16, No. 1, January 1991, pp. 152–162.

[9] T. M. Lam, M. Mulder, and M. M. Van Paassen, "Haptic feedback for UAV tele-operation - Force offset and spring load modification," in *IEEE International Conference on Systems, Man and Cybernetics*, Tapei, Tawain, 8-11 October 2006, pp. 1618–1623.

[10] D. A. Abbink and M. Mulder, "Exploring the dimensions of haptic feedback support in manual control," *Journal of Computing and Information Science In Engineering*, Vol. 9, No. 1, 2009, pp. 011 006–1 – 011 006–9.

[11] J. Lasschuit, "Modeling the neuromuscular system dynamics for haptic interface design," Delft, The Netherlands," Unpublished Msc. Thesis, 2007.

[12] S. G. Hart and L. E. Staveland, "Development of NASA-TLX (Task Load Index): Results of empirical and theoretical research," in *Human Mental Workload*, P. A. Hancock and N. Meshkati, Eds. Elsevier Science Publishers (North-Holland), 1988, pp. 139–183.